Published in final edited form as:
Immunity. 2013 January 24; 38(1): 92–105. doi:10.1016/j.immuni.2012.11.005.

Interferon-Inducible Cholesterol-25-Hydroxylase Broadly Inhibits Viral Entry by Production of 25-Hydroxycholesterol

Su-Yang Liu[1,†], **Roghiyh Aliyari**[1,†], **Kelechi Chikere**[1], **Guangming Li**[4], **Matthew D. Marsden**[1,2], **Jennifer K. Smith**[5], **Olivier Pernet**[1], **Haitao Guo**[4], **Rebecca Nusbaum**[5], **Jerome A. Zack**[1,2], **Alexander N. Freiberg**[5], **Lishan Su**[4], **Benhur Lee**[1,2,3], and **Genhong Cheng**[1,*]

[1]Department of Microbiology, Immunology, and Molecular Genetics. University of California, Los Angeles, CA USA

[2]UCLA AIDS Institute, UCLA, Los Angeles, CA, USA

[3]Department of Pathology and Laboratory Medicine, UCLA, Los Angeles, CA, USA

[4]Lineberger Comprehensive Cancer Center, School of Medicine, University of North Carolina at Chapel Hill, Chapel Hill, NC, USA

[5]Department of Pathology, University of Texas, Medical Branch, Galveston, TX, USA

SUMMARY

Interferons (IFN) are essential antiviral cytokines that establish the cellular antiviral state through upregulation of hundreds of interferon-stimulated genes (ISGs), most of which have uncharacterized functions and mechanisms. We identified Cholesterol-25-hydroxylase (Ch25h) as an antiviral ISG that can convert cholesterol to a soluble antiviral factor, 25-hydroxycholesterol (25HC). Ch25h expression or 25HC treatment in cultured cells broadly inhibits enveloped viruses including VSV, HSV, HIV, and MHV68 as well as acutely pathogenic EBOV, RVFV, RSSEV, and Nipah viruses under BSL4 conditions. As a soluble oxysterol, 25HC inhibits viral entry by blocking membrane fusion between virus and cell. In animal models, Ch25h-knockout mice were more susceptible to MHV68 lytic infection. Moreover, administration of 25HC in humanized mice suppressed HIV replication and rescued T-cell depletion. Thus, our studies demonstrate a unique mechanism by which IFN achieves its antiviral state through the production of a natural oxysterol to inhibit viral entry and implicate membrane-modifying oxysterols as potential antiviral therapeutics.

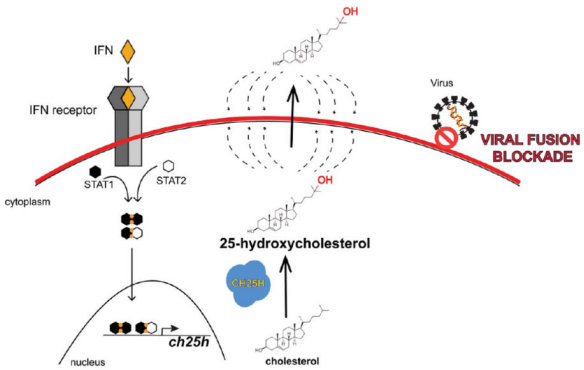

*Corresponding Author, Genhong Cheng, gcheng@mednet.ucla.edu, 615 Charles E. Young Dr. S., Biomedical Science Research Building, Rm. 210A, Los Angeles, CA 90095, 310-825-8896.
†These authors contributed equally to this work

INTRODUCTION

Viruses are obligate intracellular pathogens that—despite having unique structure and function--undergo lifecycle stages of entry, replication, protein synthesis, assembly, and egress. Upon specific binding to cell surface molecules, non-enveloped virus can enter the cell directly while enveloped viruses undergo a fusion process that requires specific interactions between the viral and cellular receptors and membranes. After entry, viral components are released into the cytoplasm and may enter the nucleus. Although incipient viral proteins may be sufficient to initiate early lifecycle processes, full viral replication, transcription and translation require utilization of cellular factors. The newly synthesized viral proteins and genome are then coordinately assembled into virions, which then exit the cell by lysis or budding.

While viruses exploit host factors to successfully replicate, the innate immune system produces interferons (IFN), essential antiviral cytokines that induce wide array of antiviral effectors. Individually, many of these IFN-stimulated genes (ISGs) work to inhibit virus at particular stages of its lifecycle. IFITM proteins block viral entry and ISG20, a 3–5' exonuclease, degrades single stranded viral RNA; PKR inhibits viral translation through suppression of eIF2a elongation factors and tetherin prevents release of virions from the cell (Degols et al., June; García et al., 2006; Neil et al., 2008; Van Damme et al., 2008; Brass et al., 2009). These ISGs exemplifies only a few of the hundreds of confirmed ISGs; most of them are uncharacterized.

Cholesterol-25-hydroxylase (Ch25h) is an ISG conserved across mammalian species. The intronless gene encodes an endoplasmic-reticulum-associated enzyme that catalyzes oxidation of cholesterol to 25-hydroxycholesterol (25HC)(Holmes et al., 2011). 25HC belongs to a diverse class of endogenous oxysterols, the oxidation products of cholesterol. It is widely understood to be a soluble factor that controls sterol biosynthesis through regulation of sterol-responsive element binding proteins (SREBP) and nuclear receptors (Kandutsch et al., 1978; Janowski et al., 1999). While oxysterols have unique roles in metabolism, studies have implicated their importance in immunity. Macrophages and dendritic cells express Ch25h robustly in response to various toll-like receptor (TLR) ligands and IFN (Bauman et al., 2009; Park and Scott, 2010). Ch25h suppresses IgA production in B-Cells and may promote intracellular bacterial growth by induction of prosurvival factors in macrophages (Bauman et al., 2009; Zou et al., 2011). Like immune mediators, dysregulation of 25HC is associated with immune pathology such as atherosclerosis (Andrew J and Jessup, 1999), which is partly attributed to its induction of the inflammatory cytokine, IL-8 (Wang et al., 2012). Although these studies support a conserved immunological role of Ch25h and 25HC, their functions in the antiviral immune response remain elusive.

We have found that Ch25h is important for the host immune response against viral infection. This study explores the antiviral properties of Ch25h, the mechanism of its viral inhibition, as well as its physiological significance during viral infections.

RESULTS

Ch25h is an IFN-dependent Gene with Antiviral Activity

In a microarray analysis of IFNα and IFNγ stimulated murine bone marrow-derived macrophages (BMMs), we found both types of IFNs induced expression of Ch25h within 3hrs (Fig. 1A). Gene expression analysis by qPCR showed that Ch25h is induced by polyI:C (TLR3 agonist) in BMMs and dendritic cells; BMMs had higher induction in response to IFN (Fig. 1B upper panel). In mice infected with 5^6 pfu of VSV i.p., Ch25h was induced

after 18 and 36h in lung, liver, and kidney, with highest induction in liver and kidneys (Fig. 1B lower panel). An RNAseq analysis showed toll-like receptor 4 (TLR4) induction of Ch25h was dependent on IFN receptor (IFNAR) but independent of IL-27, a cytokine that mediates IFN secondary gene expression, such as IL-10 (Fig. 1C). This result was confirmed by qPCR showing that Ch25h expression was induced by TLR2, 3, 4, and 9 agonists, with highest expression induced by polyI:C (TLR3) and lipidA (TLR4). IFN receptor deficient (*ifnar−/−*) BMMs had abrogated Ch25h expression when treated with these agonists showing that Ch25h expression is IFN-dependent (Fig. 1D).

In a previous study, we performed a blinded, unbiased screen for antiviral ISGs against vesicular stomatitis virus co-expressing GFP (VSV-GFP) (Liu et al., 2012). We co-transfected individual plasmids encoding an ISG with a plasmid encoding a red fluorescent protein, DsRed. Transfection proceeded for 36h before infection with VSV-GFP. At 9hpi, we quantified VSV-GFP with FACs by gating on DsRed-positive population, which are cells that highly express the ISG (Fig 1. E). Expression of Ch25h inhibited VSV-GFP replication by ~89% at 9hpi (Fig 1. F). IFN activators like Tbk1, Ifih1, and Irf1 strongly inhibited VSV as well as the RNA exonuclease, ISG20. To validate the antiviral effect of Ch25h, we generated a doxycycline-inducible Ch25h-flag construct co-expressing a flourescent-red mCherry (Ch25h-mCherry). Doxycycline addition to HEK293T expressing this construct increased CH25H-flag expression (Fig. 2A top) and mCherry expression in a dose-dependent manner (Fig 2A, bottom). When infected with VSV-GFP, HEK293T expressing Ch25h-mCherry and treated with doxycycline exhibited a dose-dependent inhibition of VSV-GFP compared to vector control (Fig 2A, bottom). Taken together, Ch25h is sufficient to inhibit VSV.

Loss of function of Ch25h leads to Susceptibility to Viral Infections *in vitro*

We sought to determine whether Ch25h might play a necessary role in the viral infection. We generated Ch25h stable knockdown cell lines from murine macrophage cell line, RAW264.7, with two distinct shRNA sequences against Ch25h and confirmed the knockdown by qPCR (Fig. 2B). Both knockdown cell lines demonstrated increased VSV replication compared to scramble control (Fig. 2C). To further validate these results, macrophage and B-cell lines were derived from Ch25h-deficient (*ch25h−/−*) and matching wild-type (*ch25h+/+*) mice. In our conditions, we could not establish VSV infection in primary cell lines; hence we immortalized BMMs and B-cells with J2 and BCR-ABL oncogenic retroviruses, respectively. *Ch25h−/−* J2 BMMs displayed 5-fold increased susceptibility to VSV infection compared to *ch25h+/+* J2 BMMs at 14hpi. In B-cells transformed with BCR-ABL, we observed about 100 fold increase in VSV-GFP replication in 3 different *Ch25h−/−* B-Cell clones at 48hpi compared to 2 *ch25h+/+* B-cell clones (Fig. 2E). These results show that Ch25h may be required for host antiviral immunity.

Ch25h produces a soluble antiviral factor that is not IFN

In overexpression studies described in Fig. 1, HEK293T were transfected with ISG plasmids and DsRed in 3:1 ratio such that DsRed-positive cells (DsRed+) should represent cells that highly expressed the ISG, whereas DsRed-negative (DsRed-) cells should represent low ISG expressers (Fig. 3A). IFN activators, Tbk1, Irf1, and Ifih1, inhibited VSV-GFP expression in both populations showing DsRed+ cells confer viral resistance to DsRed-through a soluble factor, which is IFN (Fig. 3B). In contrast, the cytoplasmic viral RNA exonuclease, ISG20, only inhibited VSV growth in DsRed+ population, but not DsRed-population. Overexpression of Ch25h also inhibited virus in both DsRed+ and DsRed-populations suggesting that Ch25h produced a soluble factor that act *in trans* to confer antiviral activity onto other cells.

To determine if Ch25h produced a soluble antiviral factor, we tested whether conditioned medium from cells overexpressing Ch25h had antiviral activity. HEK293T cells were transfected with vector, interferon activators (Tbk11, Irf1, and Ifih1), Ch25h, or ISG20, and the conditioned media was transferred onto freshly plated HEK293T cells for 8h before infection with VSV-GFP (0.01MOI). As expected, conditioned media from IFN activators inhibited VSV growth, but not ISG20 (Fig. 3 C). Conditioned medium from Ch25h generated ~60% VSV-GFP inhibition. We have also observed similar effect in several human and murine cell lines including HeLa, 3T3, BHK, Veros, MDCK, and Huh751 (Supp. Fig. S1A). These results demonstrate that Ch25h produces a soluble antiviral factor.

IFN induces many ISGs that positively feedback and amplify its production, leading to the hypothesis that Ch25h-induced soluble factor is IFN. Ch25h conditioned medium, however, had no detectable IFNβ by ELISA and did not induce an IFN-stimulated responsive element (ISRE) luciferase reporter (Supp. Fig. S1 B and C). More importantly, Ch25h-conditioned medium inhibited VSV replication in both *ifnar−/−* fibroblasts and J2 BMMs. As positive control, conditioned media from IFN activators, Irf1, Ifih1, and Rig-I, were unable to confer antiviral activity to *ifnar−/−* cell lines (Fig. 3 E and F). Taken together, Ch25h produces a soluble factor that is not IFN and can confer antiviral activity independent of IFN.

25-hydroxycholesterol (25HC), the product of CH25H, has antiviral activity

Ch25h catalyzes oxidation of cholesterol to 25-hydroxycholesterol (25HC), a soluble oxysterol that acts as an autocine and paracrine mediator (Fig. 4 A, top). We hypothesized that the soluble antiviral factor generated by Ch25h is 25HC. Treatment of HEK293T cells with 25HC for 8h inhibited VSV-GFP expression by FACs in a dose-dependent manner with IC_{50} of ~1μM (Fig. 4 A, bottom). Two other oxysterols, 22-(R)-hydroxycholesterol (22R-HC) and 22-(S)-hydroxycholesterol (22S-HC), had no effect on VSV. 22R-HC is also an agonist for the nuclear hormone receptor LXR and 22S-HC is an inactive ligand. Since 25HC has been implicated as a LXR agonist, these results also suggest that the antiviral effect was LXR-independent. In addition, 25HC treatment of *ch25h+/+* and *ch25h−/−* J2 BMMs reduced VSV replication (Fig. 4B).

The effect of 25HC on cell viability and toxicity was also assessed. 25HC treatment at 10 times IC_{50} (10μM) did not increase LDH in supernatants of cells after 16h of treatment; LDH level increased only after 30–40h treatment at 40μM of 25HC (Supp. Fig. S2A and B). Similarly, Ch25h-conditioned medium did not alter cell viability as measured by cellular ATP levels (Supp. Fig. S2C). Therefore, these results suggest that the antiviral activity of Ch25h is carried out through its enzymatic product, 25HC, which has specific antiviral effect.

CH25H and 25HC are broadly antiviral

To determine the breadth of antiviral activity of Ch25h, we tested the effect of Ch25h-conditioned medium and 25HC on various viruses. For HIV, primary peripheral blood mononuclear cells (PBMCs) were treated with conditioned medium or oxysterol and subsequently infected with HIV NL4-3. At 3dpi, Ch25h- and Irf1-conditioned media caused ~75% reduction of HIV NL4-3 p24 expression (Fig. 4C). Similarly, 25HC (1μM) inhibited p24 expression by ~80% at 3dpi compared to vehicle treatment, whereas 22S-HC had no effect (Fig. 4D). Ch25h-conditioned medium also inhibited herpes simplex virus 1 (HSV-1) by plaque assay (Fig. 4E) and expression of Ch25h in HEK293T also reduced murine gammaherpes virus (MHV68) infection by plaque assay (Fig. 4F).

HIV, HSV-1, and MHV68 are viruses that achieve chronically persistent infections. To determine whether Ch25h-induced 25HC can inhibit acutely pathogenic viruses, we tested

the effect of 25HC on live Ebola virus (EBOV-Zaire), Nipah virus (Bangladesh), Russian Spring-Summer Encephalitis Virus (RSSEV), and Rift Valley fever virus RVFV (wild-type strain ZH501 and vaccine strain MP12) under BSL4 conditions. Figures 4 G, H, I, and J show that 1μM of 25HC inhibited replication of these live viruses. 25HC also inhibited replication of Nipah and RVFV (MP12) in a dose-dependent manner (Supp. Fig. S2 D and E). In contrast, a non-enveloped virus, adenovirus coexpressing GFP, was not affected by 25HC as measured by FACs (Fig. 4K). Taken together, Ch25h-induced 25HC has antiviral activity against several types of enveloped DNA and RNA viruses, while it does not affect a non-enveloped virus.

25HC inhibits VSV entry

We took advantage of tools available for VSV and HIV to study the mechanism of Ch25h inhibition on the viral lifecycle. First, we utilized the pseudotyped VSVΔG-Luc reporter virus system that has the receptor-binding G gene (VSV-G) replaced with a luciferase reporter gene that is capable of single-round infection (Negrete et al., 2006). Quantification of luciferase activity is indicative of viral lifecycle processes from entry to protein synthesis. Ch25h- and Irf1-conditioned media inhibited VSVΔG-Luc expression suggesting inhibition of viral replication at an early stage (Fig. 5A). In a time-of-addition experiment, longer pre-treatment times correlated with greater inhibition of VSVΔG-Luc expression, compared to vehicle treated controls (Fig. 5B). These results suggest that 25HC does not inhibit VSV during infection or after infection has taken place. Rather, it is likely that 25HC establishes an antiviral state prior to infection.

Since these data implicate early viral lifecycle steps may be affected, we carried out experiments to determine whether 25HC affects attachment (Weidner et al., 2010). HEK293Ts were treated for 8h with ethanol (EtOH), 25HC (1μM), CPZ (10μg/mL), an endocytosis inhibitor that would have no effect on binding. To measure binding, VSV (1MOI) was incubated with HEK293T at 4°C for 1h to allow for binding but not cell entry. After washing 3 times with cold PBS, quantification of VSV genomic RNA (gRNA) showed that 25HC did not inhibit viral binding significantly ($P>0.05$) (Fig. 5C).

To determine if 25HC affects efficiency of fusion, we established a VSV-G β-lactamase (βla) entry assay based on the ability of VSV-G to be pseudotyped onto viral-like particles made from the Bla-Nipah virus matrix fusion protein, herein called VSV-G/βlaM (Wolf et al., 2009). VSV-G mediated fusion will result in cytoplasmic delivery of Bla-M; by addition of lipophilic fluorescent CCF2-AM substrate, the βla activity can be measured by the green (525nm) to blue (485 nm) fluorescence shift as a result of CCF2-AM cleavage (Zlokarnik et al., 1998). Hence, efficiency of virus-cell fusion can be measured by the increase in the ratio of blue to green (blue:green) fluorescence, which is reflective of the βla activity associated with βlaM that was been released into the cytoplasm after VSV-G mediated fusion (Cavrois et al., 2002; Wolf et al., 2009). Unlike the VSVΔG-Luc pseudotyped virus, this VSV-G/βlaM entry assay does not require transcription and translation of viral proteins for reporter gene expression. Fusion is proportional to βlaM concentration, which is estimated by the rate constant (k) derived from the slope of the reaction during the linear phase of the reaction within the first hour.

HEK293T cells were transfected with several ISGs for 48 hours and infected with VSV-G/βlaM. Figure 5D showed that Ch25h reduced efficiency of VSV fusion. Compared to vector control, βlaM activity from Ch25h-transfected cells proceeded 48% of vector-transfected cell (compare rate constants in inset table) and plateaued at a lower level. The previously described entry inhibitor, Ifitm3, also reduced VSV-G/βlaM fusion (Brass et al., 2009). ISG20, a viral RNA exonuclease, had no effect on viral entry. Irf-1 transfected cells also inhibited fusion, presumably by up-regulation of IFN. To show this, we separately

confirmed that recombinant IFN inhibited VSV-G/βlaM fusion (Supp. Fig. 3A). Ch25h-conditioned medium similarly inhibited VSV-G/βlaM entry, with a more pronounced effect than Irf1-conditioned medium (Fig. 5E). Furthermore, treatment of 25HC at 1, 2.5, and 5μM inhibited VSV-G/βlaM activity, by 44%, 56%, and 70%, respectively (Fig. 5F). These results demonstrate that the IFN, Ch25h, and its cognate product, 25HC, modulates the target cell membrane in a manner that inhibits efficiency of virus-cell fusion.

Since the viral entry step involves interactions between both the viral and cellular membranes, we then asked if the infectivity of the virions were affected when produced from 25HC treated cells. HEK293T were treated with and without 25HC (2.5μM) for 8h and infected with live VSV at 0.01 MOI for 1h. The cells were treated as before for 24h. Viral superntants were then purified by ultracentrifugation through a 20% sucrose cushion, which removed any residual 25HC. As expected, there was >60% reduction in the amount of VSV from 25HC treated samples versus control, as measured by qPCR for the number of viral genome copies (gRNA) (Supp. Fig. 3B). To assess infectivity, we normalized viral titer from 25HC- or vehicle-treated cells based on gRNA and determined infectivity by plaque assay. After normalization, VSV from 25HC-treated cells formed equivalent PFU titer as viruses from vehicle-treated cells (Supp. Fig. 3C). These results show that 25HC exerts its antiviral effect by altering target cell membrane properties and does not alter membrane of virions produced from those cells.

25-hydroxycholesterol is a suppressor of SREBP2, which controls sterol biosynthesis and can alter membrane sterol composition. Hence, we tested the hypothesis that 25HC inhibits viral growth through suppression of SREBP2. We tested whether overexpression of active (cleaved) form of SREBPs in HEK293T would overcome the anti-viral effect of 25HC. Overexpression of active forms of SREBP1a, SREBP1-c, and SREBP2 in HEK293Ts, however, did not reverse 25HC antiviral effect (Supp Fig. S4A). These data demonstrate that the antiviral effect of 25HC is SREBP independent.

25HC is known to down-regulate numerous sterol biosynthetic enzymes including HMG-CoA reductase, which produces the key intermediate mevalonate (Pezacki et al., 2009) (Supp. Fig. S4B). We hypothesized that mevalonate may reverse the antiviral effect of 25HC. Addition of exogenous mevalonate (300μM) to HEK293T before and during 25HC treatment, however, did not reverse the antiviral effect of 25HC (Supp Fig. S4C).

25HC also may inhibit production another intermediate isopentenyl-pyrophosphate (Isopentyl-PP), which is substrate for prenylation of proteins on CAAX motif. This post-translational modification is mediated by farsenyl-transferase (FTase) and gernylgernyl-transferase (GTase). We tested the hypothesis that inhibition of prenylation can inhibit VSV growth. HEK293T were treated with FTase and GTase inhibitors, FTI-276 and GGTI-298 (5–20μM), and infected with VSV-GFP. FTI-276 treatment had no effect on VSV, whereas GGTI-298 reduced viral growth at 10–20μM (Supp Fig. S4D). GGTI-298, however, caused >10% reduction in cell viability by ATP content, whereas 25HC and FTI had no effect (Supp Fig. S4E). Furthermore, FTI-276 and GGTI-298 did not reduce VSV fusion entry by VSV-G/βlaM assay (Supp Fig. 4F and G). Taken together, while prenylation inhibition may have some antiviral effect, it seems to inhibit cell viability and not affect the viral entry as observed with 25HC.

Ch25h and 25HC inhibits HIV entry

We sought to validate Ch25h and 25HC antiviral mechanism on HIV. Unlike VSV, HIV is a retrovirus that undergoes pH-independent cellular entry. In CEM cells, 25HC inhibited >50% luciferase expression from single round infection of pseudovirus with HIV-IIIB envelope on a NL4-3 backbone coexpressing luciferase (pNL4-3.Luc.-R-E) (Fig. 6A). AZT,

an inhibitor of reverse transcription, served as positive control and inhibited expression by ~70%. Hence, these data also suggest 25HC inhibits viral lifecycle prior or at translation.

HIV initiates reverse transcription of its genomic RNA to DNA immediately after entry. Hence, we examined the effect of 25HC on the production of full-length, reverse-transcribed DNA (lateRT). CEM cells were infected with pseudotyped HIV-IIIB and lateRT was measured by qRT-PCR. 25HC inhibited lateRT expression >99% at 2hpi and ~70% at 6hpi (Fig. 6B). The HIV entry inhibitor, AMD3100, served as a positive control. Elvitegravir is used as a negative control because it inhibits HIV at the step of DNA integration after lateRT formation. These results show that 25HC inhibits a stage of the HIV life cycle before reverse transcription of its genome.

We next asked whether Ch25h inhibits HIV similar to VSV at the level of entry. We coexpressed pNL4-3 with Bla-VPR fusion gene to produced virions containing Bla-VPR (NL4-3/Bla). CEM cells treated with Ch25h conditioned medium exhibited ~65% reduction in viral entry compared to vector- and Isg20-conditioned medium. AMD3100 abrogated NL4-3/Bla entry (Fig. 6C). We further confirmed our findings by FACS analysis and observed ~50% decrease in the number of cells expressing cleaved CCF2-AM substrate (blue population) in CEM treated with Ch25h conditioned medium compared to control (supp. Fig. S5A). Treatment of CEM cells with 25HC (5μM) for 24h caused ~60% decrease in NL4-3/Bla blue-green ratio at endpoint (Fig. 6D) and >85% reduction in cells expressing cleaved CCF2-AM by FACS analysis (Fig. 6E).

Since 25HC may have diverse cellular effects, we asked whether 25HC might affect other HIV life cycle processes. To assess 25HC effect on HIV transcription, we transfected HEK293Ts with pNL4-3 co-expressing GFP (NL4-3-GFP) and treated the cells with 25HC at 4h post transfection. The NL4-3-GFP expression after 24h was not suppressed suggesting that 25HC does not affect HIV transcription and translation (Supp. Fig. S5B). Concurrently, treatment of with 25HC did not reduce budding of HIV virions from NL4-3-GFP transfected cells as measured by HIV p24 in the supernatants, while Nelfinavir, a known protease inhibitor that reduces subsequent budding, inhibited p24 expression by >50% at 24 and 48h post transfection (Supp. Fig. S5C). Taken together, Ch25h and 25HC inhibits efficiency of HIV membrane fusion, while 25HC treatment does not seem to affect HIV transcription, translation, and budding processes.

25HC inhibits virus-cell membrane fusion

Although βla data demonstrate 25HC inhibits viral entry processes up to fusion, we sought to test whether 25HC inhibits the viral fusion process itself. Since 25HC inhibited live Nipah replication (Figure 4H), we took advantage of the robust system of Nipah fusion (F) and attachment (G) proteins to induce pH-independent cell-cell membrane fusion to form syncytias. Vero cells were transfected with recombinant Nipah F and G at equal ratios for 5h and refreshed with media containing 25HC or vehicle control. At 21h post transfection, cells were fixed and stained by Giemsa. Grossly, 25HC treatment led to less syncytia formation and fewer nuclei per syncytias compared to control (Fig. 6F). In a blinded count of numbers of nuclei per syncytia, a standard measure of fusion, 2μM of 25HC reduced fusion by ~50% and 10μM by ~60% relative to control (Fig. 6G). These data demonstrate that 25HC modifies the cellular membrane to inhibit viral membrane fusion.

25HC Directly Modifies Cell Membrane to Impede Viral Infection

We further explored whether 25HC can directly change membrane property to inhibit fusion. We hypothesized artificial liposomes with 7:3 phosphatitdylcholine:cholesterol ratio, which is similar in composition to cell membranes, would compete with the ability for 25HC

to incorporate into cell membrane. HEK293T incubated with liposome alone had no effect on viral infection while treatment of 25HC with liposomes caused a dose-dependent reversal of 25HC anti-viral inhibition (Fig. 6H). As a positive control, we demonstrated that liposome could compete with a known viral membrane fusion inhibitor, LJ001, as described previously (Wolf et al., 2010). These results show that 25HC directly modify cellular membrane to inhibit viral fusion.

25HC reduces HIV infection *in vivo*

We used HIV infection in a humanized mouse model to determine the antiviral effect of 25HC *in vivo*. Humanized NOD-Rag1^{null}Il2rg^{null} mice (NRG-hu) were administered 25HC (50mg/kg) 12h prior to infection with HIV NL4-R3A by intraperitoneal (i.p) injection. 25HC or the vehicle, 2-hydroxypropyl-β-cyclodextrin (HβCD), was administered daily and the serum was collected 7dpi. Quantification HIV RNA in the serum from 2 combined experiments showed >80% reduction of HIV RNA (copies/mL) in 25HC-treated mice compared to vehicle-treated mice ($P<0.0001$) (Fig. 7 A). At termination of the experiment on 14dpi, HIV p24 was significantly lower in CD4 T-cells from spleens of 25HC treated mice than control (Fig. 7 B). Moreover, at 10dpi, 25HC prevented HIV-mediated CD4+ T-cell depletion compared to vehicle control in CD3+(live T-cell) population in peripheral blood leukocytes ($P<0.05$); this effect was less significant in the spleen ($P=0.06$) (Fig. 7C). These data show that administration of 25HC can cause antiviral effect against HIV *in vivo*.

Ch25h-deficient mice are more susceptible to viral infections

To determine whether Ch25h has a physiological role in host defense against viral infection, we tested whether *ch25h−/−* mice had increased susceptibility to matching wild-type mice (*ch25h+/+*). Since Ch25h expression inhibited MHV68 *in vitro*, we used MHV68 coexpressing luciferase (MHV68-Luc) to infect mice so that viral lytic growth kinetics could be measured in real time by bioluminescence. Eight-week old female *ch25h+/+* and *ch25h−/−* mice (N=4 in each group) were infected with 500pfu of MHV68-Luc i.p. and imaged every day after 3dpi. Average and maximal luminescence intensities from ventral, right, left, and dorsal side of every mouse were measured. We observed significantly higher MHV68-Luc activity in *ch25h−/−* mice over *ch25h+/+* mice starting 5 dpi and maximal differences between day 7 and 8 (Fig. 7 D and E). MHV68-Luc activity began to wane in both groups by 9dpi with significantly higher activity in *Ch25h−/−* mice. To validate the imaging results, *Ch25h−/−* spleens had approximately ~3.5 fold higher MHV68 genomic DNA than spleens of *Ch25h+/+* mice at 10dpi (Fig. 7 F and G). These results show that Ch25h is a physiologically important antiviral factor.

DISCUSSION

We have identified the antiviral activity of an IFN-inducible gene, Ch25h, through a systematic, functional screen. Distinct from known IFN-mediated antiviral mechanisms, Ch25h inhibits growth of a wide range of enveloped viruses by production of a soluble oxysterol, 25-hydroxycholesterol. It also exemplifies the only soluble antiviral ISG that is not IFN itself. Independent of its known regulatory effect on metabolism, 25HC impairs viral entry at the step virus-cell fusion by inducing cellular membrane changes. In animal models, administration of 25HC reduces HIV infection in humanized mice. Moreover, the immune response against viral infections requires Ch25h *in vivo*. These findings illustrate an essential function of Ch25h in immunity.

This study shows an unappreciated relationship between the host IFN response and an oxysterol. While antiviral effects of some oxysterols have been documented (Moog et al., 1998; Pezacki et al., 2009), we have found 25HC broadly inhibits viral membrane fusion,

which is not specific to particular structural classes of fusion proteins. For example, HIV and Ebola have class-I fusion peptides, RVFV and RSSEV use class-II peptides, whereas VSV and HSV belong to class III ((Kielian and Rey, 2006; Vaney and Rey, 2011). 25HC is also antiviral against viruses that undergo either pHdependent or pH-independent fusion as exemplified by VSV and HIV, respectively. These findings suggest that 25HC affects a more basic fusion process involving the viral and cellular membrane.

Since 25HC can permeate through membranes, 25HC may directly change cellular membranes to exert its antiviral effect. In the present study, incubation of liposomes and 25HC reverses the antiviral effect of 25HC suggesting liposomes take up 25HC and decrease its active concentration. Literatures support the membrane modifying effect of 25HC. First, it increases cellular cholesterol accessibility by directly mobilizing cholesterol from membranes and consequently prevent condensing effects of cholesterol (Lange et al., 1995; Olsen et al., 2011). Secondly, 25HC affects solvent exposure of phospholipid head groups in artificial membranes (Gale et al., 2009). One model suggests that while membrane cholesterol adopts parallel orientation to adjacent acyl chains, 25HC adopts a tilted position in the membrane because of its hydroxyl group, which may lead to membrane expansion effects. We also hypothesize that the hydrophilic interactions of the hydroxyl groups of 25HC lead to aggregation in the membrane. These perturbations could affect viral-cellular fusion, which is fundamentally dependent on membrane properties such as spacing of lipid head groups, receptor accessibility, membrane curvature, and fluidity (Pécheur et al., 1998; Teissier and Pécheur, 2007). Studies on viral entry have predominantly focused on viral fusion components and their interactions with specific cellular receptors. How membrane properties modulate viral fusion remains subject of further research.

Our data suggest viral entry is a point of viral growth inhibition by Ch25h and 25HC under the conditions described, which are generally 8–16h pre-treatment with 1–10μM of 25HC in standard growth medium. Given the expanding role of oxysterol functions, other antiviral mechanisms may exist and manifest under particular conditions or with certain types of viruses. Of note, the inhibition of live VSV-GFP is more pronounced than VSV-G/βlaM fusion when Ch25h is overexpressed in HEK293T, about ~85% and ~51% respectively (compare Figs. 1E and 5D). In Ch25h-conditioned medium or 25HC treated cells, the amount of reduction was comparable, ranging about 55–70% (Fig. 3C and 5E or 4A and 5F). One interpretation is that CH25H protein may have addition antiviral mechanisms than 25HC, perhaps through its association with the endoplasmic reticulum. Secondly, inhibition of geranylation with GGTI-298 led to reduced VSV growth concomitant with decreased cell viability and no effect on fusion. These results encourage further study in other antiviral mechanisms of Ch25h and 25HC.

This study provides further understanding to the intricate connection of IFN and metabolism. Although 25HC have been associated with pathological conditions like atherosclerosis and Alzheimers, our study show it plays a beneficial role in host immunity against viral infections. These results encourage the exploration of antiviral oxysterols or cellular membrane modifiers as viral entry inhibitors against acute infections.

MATERIALS AND METHODS

Cells and Reagents (Supp. Methods)

VSV, HSV, and MHV68 Viral Plaque Assay—HEK293T and RAW264.7 were infected with VSV-GFP at 0.01 MOI for 1h and the media was changed with fresh media. For J2 BMMs and BCR-ABL B-cells, 1MOI VSV-GFP was used. Approximately 150μL of supernatants were collected at various times between 8–16hpi for plaque assay. For HSV

and MHV68, 0.25MOI was used for infection and supernatants were collected at 24hpi. Titers were measured by standard plaque assays. (Supp. Methods)

HIV Infections in hPBMCs (Supp. Methods)

Ebola, RSSEV, Nipah and RVFV Infections—HeLa cells were pre-treated with 25HC (1μM) or EtOH containing medium for indicated times prior to infection with 0.1MOI of Ebola-Zaire-GFP (EBOV) or RVFV (wild type strain ZH501 or vaccine strain MP12), Nipah virus (Bangladesh), or RSSEV (Sofjin). Cell culture supernatant pooled from biological triplicates at indicated timepoints, prior virus titration by plaque assay. Titers were measured by standard plaque assays (Supp. Methods)

VSV-G/βlaM Infection—VSV-G/βlaM was produced as previously described and detaild in Supp. Methods (Wolf et al., 2009). HEK293Ts were treated with 25HC and EtOH as before and infected with VSV-G/βlaM at the empirically determined concentration for 1h. Cells were washed and CCF2-AM was added according to manufactue's protocol (Invitrogen).

NL4-3 VPR-βlaM Infection of CEM cells—CEMs cells were treated with 25HC or EtOH for a minimum of six hours and AMD3100 (20μM) for 15 minutes before infection with concentrated NL4-3 βlaM or Bald virus. Infections were spin inoculated for 60 minutes at 2,000RPM, and incubated for 2 hours at 37C. After washing, CCF2-AM (Invitrogen) was added according to manufacture's protocol. Kinetic readings were taken for 4 hours. After the kinetic reading, the cells were washed with FACS Buffer, fixed with 2 % paraformaldehyde and examined by FACs. Data was analyzed using FlowJo (Tree Star Inc.).

Nipah Fusion Assay—Vero cells were plated in 6-well dish at 5×10^5 per well overnight and transfected with 0.5μg of expression plasmids encoding Nipah F and G in OptiMEM (Invitrogen). At 5h post transfection, media was changed to DMEM (10%FBS) with or with out 25HC at the indicated concentrations. The cells were fixed by methanol 21h after transfection for 10min, stained with Giemsa stain for 2h, and decolorized with 95% ethanol. Nuclei inside syncytia were counted under light microscopy. Syncytia were defined as four or more nuclei within a common cell membrane. Relative fusion was defined by normalizing the number of nuclei per syncytia formed under the experimental conditions to that formed by in vehicle (ethanol) treated cells, which was set at 100%.

Liposome Competition Assay (Supp. Methods)

HIV infection in NRG-hu mice—NOD-Rag1^{null}Il2rg^{null} (NRG-hu) mice with stable human leukocyte reconstitution were administered 25HC (50mg/kg) or the vehicle control (HBCD) by *i.p.* injection for 12h before infection with HIV NL4-R3A (5ng of p24/mouse) or mock supernatant by intravenously injection (i.v.). Mice were administered equal amount of 25HC or HBCD every day. HIV replication (genome copy/ml in the plasma) was measured by qRT-PCR or by p24 intracellular staining (Supp. methods).

Mouse Infections and Bioluminescence Imaging—C57BL/6 and *ch25h−/−* mice were purchased from Jackson. MHV68 (500 pfu) in 200μL of PBS was administered by i.p. On days 3 following infection, mice were imaged using the *in vivo* imaging system (IVIS, Xenogen) (Supp. Methods). At 9dpi, mice were euthanized the spleens were extracted and homogenized in DMEM. Total DNA was extracted using DNeasy Blood & Tissue Kit (Qiagen) and MHV68 DNA was quantified by qRT-PCR

Statistics—For comparison of different experimental conditions at one time point, student's t-test with unpaired, 2-tailed hypothesis was used. For kinetic assays, two-way ANOVA with repeated measures was used.

Supplementary Material

Refer to Web version on PubMed Central for supplementary material.

Acknowledgments

We thank David Russell (UT Southwestern) for providing ch25h−/− bone marrow cells, and Drs. Elizabeth Tarling, Peter Edwards, and Steven Bensinger at UCLA for SREBP plasmids. We thank Gayle Boxx and Shankar Iyer for access to experimental samples and RNAseq data and Dr. Robert Modlin for his editorial advice. This project was funded NIH Grants R01 AI078389 and AI069120, Tumor Immunology Training Grant, and the Warsaw Fellowship.

REFERENCES

Andrew J, Jessup W. Oxysterols and atherosclerosis. Atherosclerosis. 1999; 142:1–28. [PubMed: 9920502]

Bauman DR, Bitmansour AD, McDonald JG, Thompson BM, Liang G, Russell DW. 25-Hydroxycholesterol secreted by macrophages in response to Toll-like receptor activation suppresses immunoglobulin A production. Proceedings of the National Academy of Sciences. 2009; 106:16764–16769.

Brass AL, Huang I-C, Benita Y, John SP, Krishnan MN, Feeley EM, Ryan BJ, Weyer JL, van der Weyden L, Fikrig E, et al. The IFITM Proteins Mediate Cellular Resistance to Influenza A H1N1 Virus, West Nile Virus, and Dengue Virus. Cell. 2009; 139:1243–1254. [PubMed: 20064371]

Cavrois M, de Noronha C, Greene WC. A sensitive and specific enzyme-based assay detecting HIV-1 virion fusion in primary T lymphocytes. Nat Biotech. 2002; 20:1151–1154.

Van Damme N, Goff D, Katsura C, Jorgenson RL, Mitchell R, Johnson MC, Stephens EB, Guatelli J. The Interferon-Induced Protein BST-2 Restricts HIV-1 Release and Is Downregulated from the Cell Surface by the Viral Vpu Protein. Cell Host Microbe. 2008; 3:245–252. [PubMed: 18342597]

Degols G, Eldin P, Mechti N. ISG20, an actor of the innate immune response. Biochimie. Jun.89:831–835. [PubMed: 17445960]

Gale SE, Westover EJ, Dudley N, Krishnan K, Merlin S, Scherrer DE, Han X, Zhai X, Brockman HL, Brown RE, et al. Side Chain Oxygenated Cholesterol Regulates Cellular Cholesterol Homeostasis through Direct Sterol-Membrane Interactions. Journal of Biological Chemistry. 2009; 284:1755–1764. [PubMed: 18996837]

García MA, Gil J, Ventoso I, Guerra S, Domingo E, Rivas C, Esteban M. Impact of Protein Kinase PKR in Cell Biology: from Antiviral to Antiproliferative Action. Microbiology and Molecular Biology Reviews. 2006; 70:1032–1060. [PubMed: 17158706]

Holmes R, VandeBerg J, Cox L. Genomics and proteomics of vertebrate cholesterol ester lipase (*LIPA*) and cholesterol 25-hydroxylase (*CH25H*). Biotech. 2011; 1:99–109. 3.

Janowski BA, Grogan MJ, Jones SA, Wisely GB, Kliewer SA, Corey EJ, Mangelsdorf DJ. Structural requirements of ligands for the oxysterol liver X receptors LXRα and LXRβ. Proceedings of the National Academy of Sciences. 1999; 96:266–271.

Kandutsch A, Chen H, Heiniger H. Biological activity of some oxygenated sterols. Science. 1978; 201:498–501. [PubMed: 663671]

Kielian M, Rey FA. Virus membrane-fusion proteins: more than one way to make a hairpin. Nat Rev Micro. 2006; 4:67–76.

Lange Y, Ye J, Strebel F. Movement of 25-hydroxycholesterol from the plasma membrane to the rough endoplasmic reticulum in cultured hepatoma cells. Journal of Lipid Research. 1995; 36:1092–1097. [PubMed: 7658157]

Liu S-Y, Sanchez DJ, Aliyari R, Lu S, Cheng G. Systematic identification of type I and type II interferon-induced antiviral factors. Proceedings of the National Academy of Sciences. 2012; 109:4239–4244.

Moog C, Aubertin A, Kim A, Luu B. Oxysterols, but not cholesterol, inhibit human immunodeficiency virus replication in vitro. Antiviral Chemistry & Chemotherapy. 1998; 9:491–496. [PubMed: 9865387]

Negrete OA, Wolf MC, Aguilar HC, Enterlein S, Wang W, Mühlberger E, Su SV, Bertolotti-Ciarlet A, Flick R, Lee B. Two Key Residues in EphrinB3 Are Critical for Its Use as an Alternative Receptor for Nipah Virus. PLoS Pathog. 2006; 2:e7. [PubMed: 16477309]

Neil SJD, Zang T, Bieniasz PD. Tetherin inhibits retrovirus release and is antagonized by HIV-1 Vpu. Nature. 2008; 451:425–430. [PubMed: 18200009]

Olsen BN, Schlesinger PH, Ory DS, Baker NA. 25-Hydroxycholesterol Increases the Availability of Cholesterol in Phospholipid Membranes. Biophysical Journal. 2011; 100:948–956. [PubMed: 21320439]

Park K, Scott AL. Cholesterol 25-hydroxylase production by dendritic cells and macrophages is regulated by type I interferons. Journal of Leukocyte Biology. 2010; 88:1081–1087. [PubMed: 20699362]

Pécheur E-I, Sainte-Marie J, Bienvenüe A, Hoekstra D. Lipid Headgroup Spacing and Peptide Penetration, but Not Peptide Oligomerization, Modulate Peptide-Induced Fusion†. Biochemistry. 1998; 38:364–373. [PubMed: 9890918]

Pezacki J, Sagan S, Tonary A, Rouleau Y, Belanger S, Supekova L, Su A. Transcriptional profiling of the effects of 25-hydroxycholesterol on human hepatocyte metabolism and the antiviral state it conveys against the hepatitis C virus. BMC Chemical Biology. 2009; 9:2. [PubMed: 19149867]

Teissier É, Pécheur E-I. Lipids as modulators of membrane fusion mediated by viral fusion proteins. European Biophysics Journal. 2007; 36:887–899. [PubMed: 17882414]

Vaney M-C, Rey FA. Class II enveloped viruses. Cellular Microbiology. 2011; 13:1451–1459. [PubMed: 21790946]

Wang F, Xia W, Liu F, Li J, Wang G, Gu J. Interferon regulator factor 1/retinoic inducible gene I (IRF1/RIG-I) axis mediates 25-hydroxycholesterol-induced interleukin-8 production in atherosclerosis. Cardiovascular Research. 2012; 93:190–199. [PubMed: 21979142]

Weidner JM, Jiang D, Pan X-B, Chang J, Block TM, Guo J-T. Interferon-Induced Cell Membrane Proteins, IFITM3 and Tetherin, Inhibit Vesicular Stomatitis Virus Infection via Distinct Mechanisms. Journal of Virology. 2010; 84:12646–12657. [PubMed: 20943977]

Wolf M, Wang Y, Freiberg A, Aguilar H, Holbrook M, Lee B. A catalytically and genetically optimized beta-lactamase-matrix based assay for sensitive, specific, and higher throughput analysis of native henipavirus entry characteristics. Virology Journal. 2009; 6:119. [PubMed: 19646266]

Wolf MC, Freiberg AN, Zhang T, Akyol-Ataman Z, Grock A, Hong PW, Li J, Watson NF, Fang AQ, Aguilar HC, et al. A broad-spectrum antiviral targeting entry of enveloped viruses. Proceedings of the National Academy of Sciences. 2010; 107:3157–3162.

Zlokarnik G, Negulescu PA, Knapp TE, Mere L, Burres N, Feng L, Whitney M, Roemer K, Tsien RY. Quantitation of Transcription and Clonal Selection of Single Living Cells with β-Lactamase as Reporter. Science. 1998; 279:84–88. [PubMed: 9417030]

Zou T, Garifulin O, Berland R, Boyartchuk VL. Listeria monocytogenes Infection Induces Prosurvival Metabolic Signaling in Macrophages. Infection and Immunity. 2011; 79:1526–1535. [PubMed: 21263022]

HIGHLIGHTS

- Ch25h inhibits virus by production of an oxysterol, 25-hydroxycholesterol (25HC)
- 25HC is a broad antiviral agent against VSV, HSV, HIV, MHV68, EBOV, NiV, RSSEV, and RVFV
- 25HC inhibits viral fusion of VSV and HIV
- *In vivo*, 25HC suppresses HIV growth and Ch25h is required for antiviral immunity

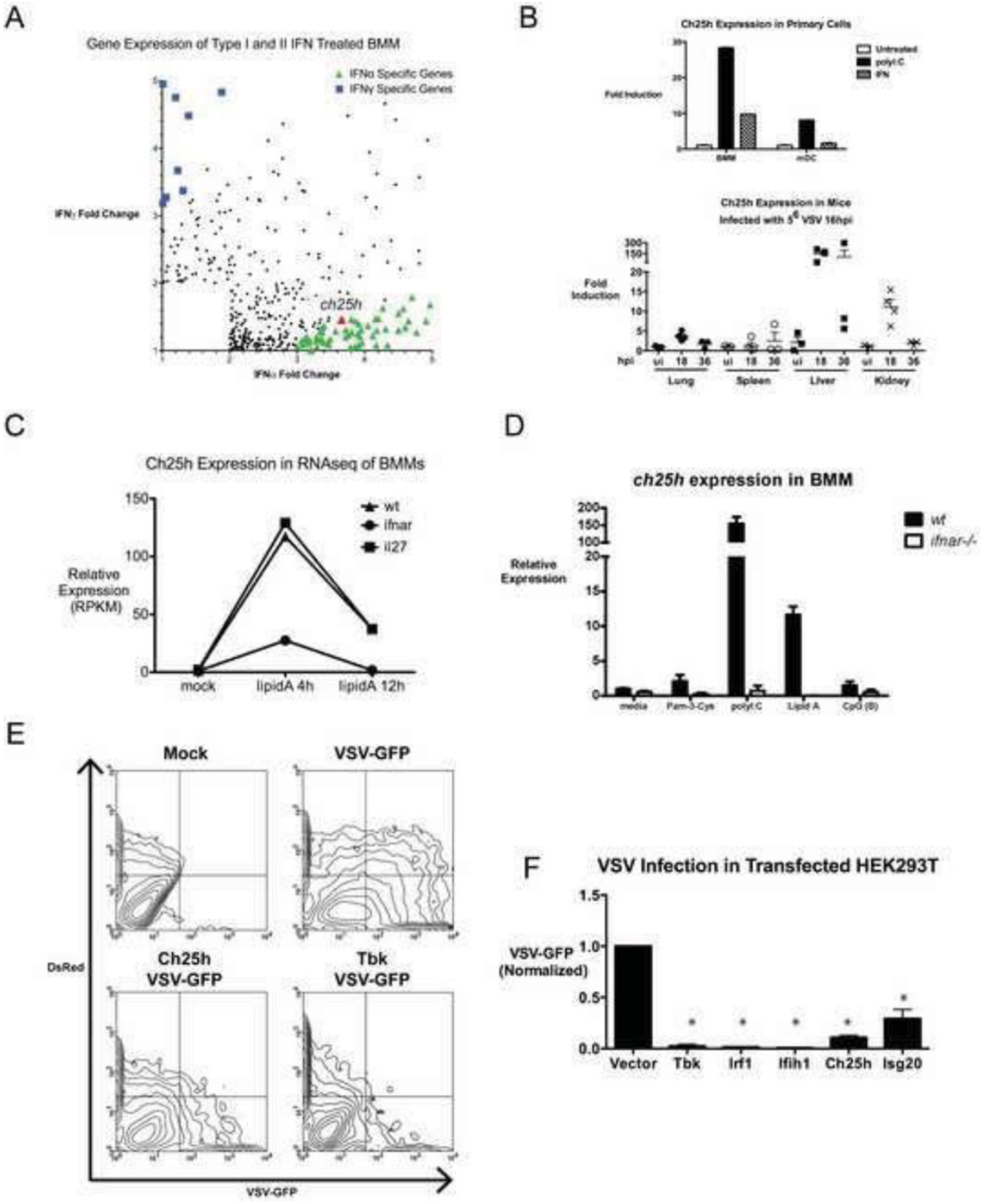

Figure 1. Ch25h is an IFN-dependent Antiviral ISG

A) Gene expression profile of BMMs treated for 2.5 h with IFNα and IFNγ at 62 U/mL and 1 U/mL, respectively. IFNα-stimulated genes that were 3-fold higher than induction of IFNγ stimulated genes were categorized as IFNα-specific (green) and vice versa for IFNγ-specific genes (blue).

B) Ch25h expression was measured by qPCR in BMMs and mDCs (top) after IFN (2000U/mL) or polyI:C(1ug/mL) treatment for 4h. Tissues from uninfected (ui) and VSV-infected C57B/6 mice were collected at indicated times (bottom).

C) Wildtype, IFNAR, and IL-27R (TCCR/WSX-1) deficient BMMs were stimulated with LipidA (100ng/mL) or saline control for 4 and 12h. Ch25h expression values are presented as RKPM values.

D) Ch25h gene expression measured by qRT-PCR of *ifnar+/+* and *ifnar−/−* BMMs stimulated with TLR agonists, Pam-3-Cys(100ng/mL), polyI:C(25ug/mL), lipidA(10ng/mL), CpG-B(100μM) for 4 hours.

E) HEK293T was co-transfected with flourescent red marker (DsRed) and with individual plasmids encoding Tbk1, Ch25h, or vector for 36h and infected with VSV-GFP (0.01MOI) for 9h. Representative contour plots are shown.

F) Similar to Part D. VSV-GFP was quantified in the DsRed-positive population normalized to vector control. VSV-GFP was defined as the product of percent GFP-positive and geometric mean of the fluorescence index (MFI). Mean±SEM; *P<0.001

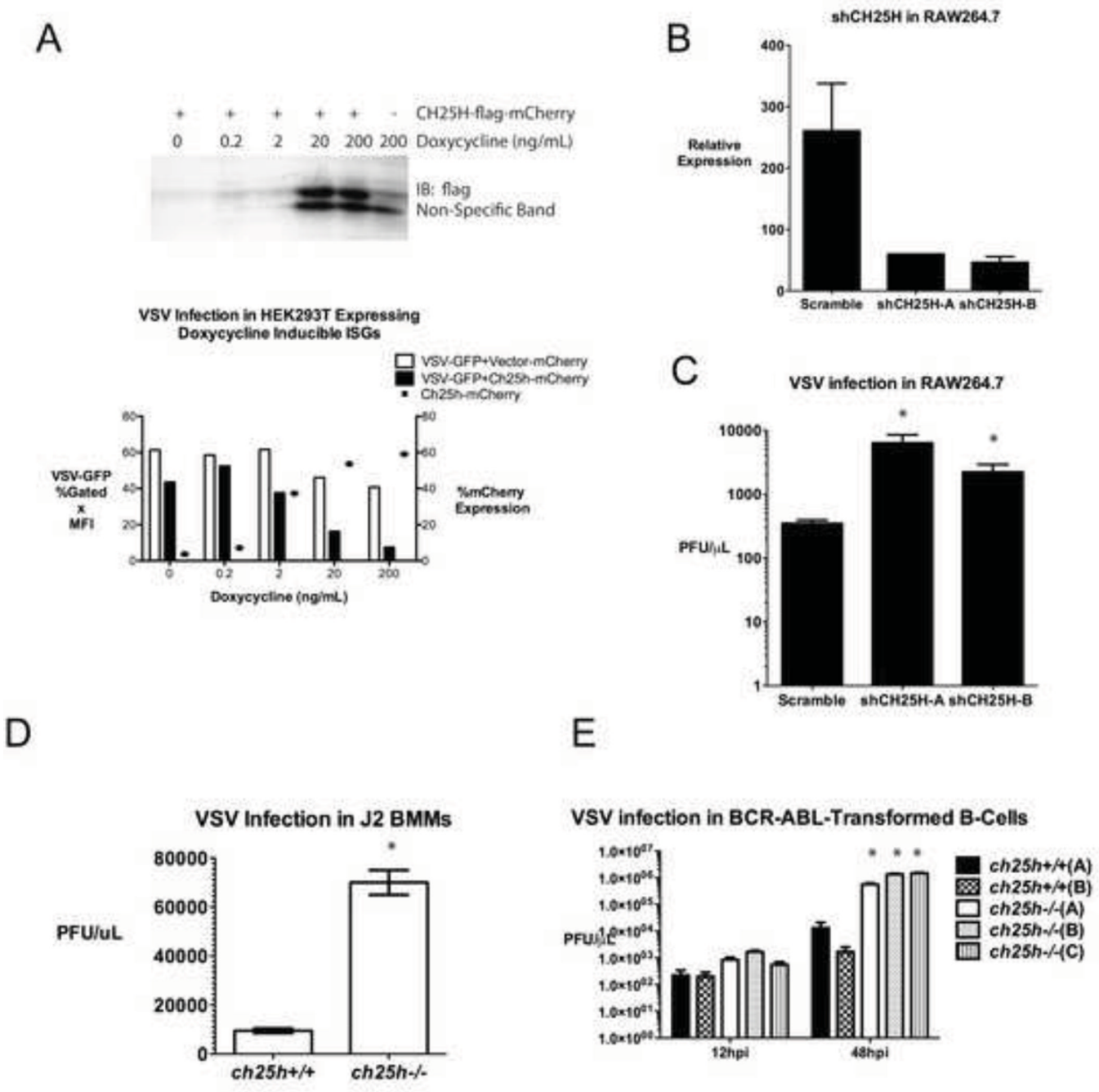

Figure 2. Ch25h-deficiency increases susceptibility to viral infection *in vitro*

A) HEK293T expressing doxycycline-inducible construct coexpressing Ch25h-flag and red flourescent marker mCherry. HEK293T was transfected with vector or Ch25h encoding plasmids for 24h and doxycycline was added for 12h at indicated concentrations. Expression of Ch25h-flag was confirmed by western blot (upper panel). After treatment, cells were infected with VSV-GFP (0.01MOI) for 9hrs and VSV-GFP was quantified by (%GFP+ X GeoMean MFI). Dots represent percent positive mCherry (lower panel).

B) RAW264.7 stably knocked down with shRNA against Ch25h were generated by retro-viral infection. Two shRNA constructs were made (shCh25h-A and shCH25h-B) along with scramble control. Knockdown was confirmed by qRT-PCR. *P<0.01

C) shCH25h-A, shCH25hB, and scrambled stable RAW264.7 were infected with VSV-GFP (0.1 MOI) and the VSV-GFP was measured by plaque assay 14hpi.
D) J2 BMM were derived from *ch25h+/+* and *ch25h−/−* mice and passaged for 2 weeks. The cells were infected VSV-GFP (0.1MOI) and viral titers 14hpi in the supernatants was quantified by plaque assay. *P<0.01
E) Individual clonal population of BCR-ABL transformed B-cells from *ch25h+/+* and *ch25h −/−* mice were infected with VSV-GFP (0.1MOI) in biological triplicates and the viral titers were measured by plaque assay at indicated times. *P<0.01

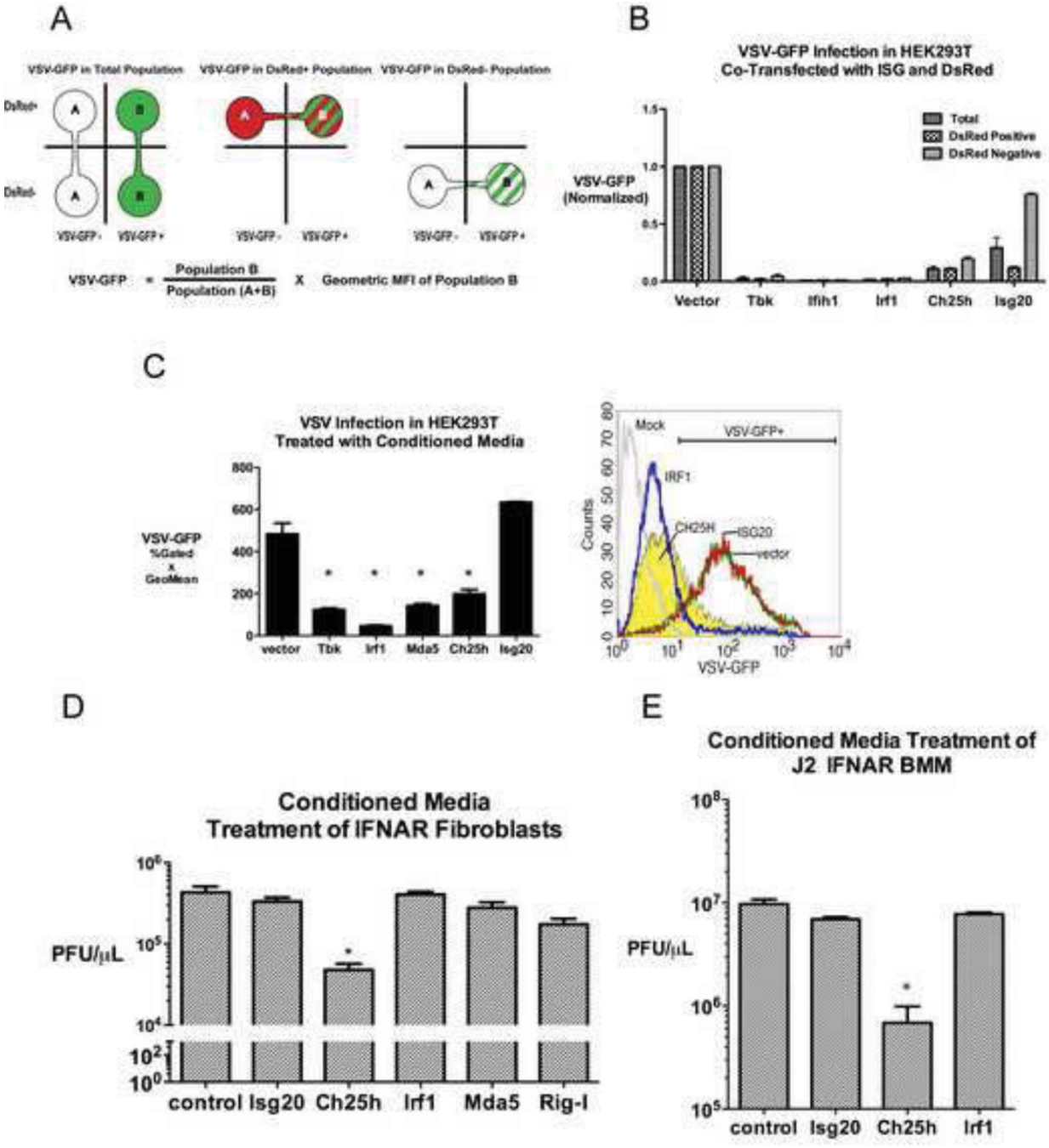

Figure 3. Ch25h produces a soluble antiviral factor that is not IFN

A) HEK293Ts were co-transfected with ISGs and DsRed as Fig. 1D. Schematic of FACs analyses of VSV-GFP in total, DsRed+, and DsRed− populations. VSV-GFP was defined as %positive GFP X geometric MFI.

B) HEK293T transfected with DsRed and indicated expression plasids were infected with VSV-GFP and analyzed by FACs as described in Fig. 3A.

C) Media collected from HEK293T after 48h transfection with indicated expression vector was treated on to freshly plated HEK293T for 8h and infected with VSV-GFP (0.01MOI) for 9h. VSV-GFP was quantified by FACs (%positive GFP X geometric MFI). Representative histogram of FACs data (right). *P<0.01

D) *Ifnar−/−* tail derived fibroblasts were treated with conditioned media for 12h from HEK293T transfected with indicated expression vector. The fibroblasts were infected with VSV-GFP (0.1 MOI) and the viral titer in the supernantant was measured by plaque assay. *P<0.05

E) *Ifnar−/−* derived J2 BMMs fibroblasts were treated with conditioned media for 12h from HEK293T transfected with indicated expression vector. The cells were infected with VSV-GFP (0.1 MOI) and the viral titer in the supernantant was measured by plaque assay. *P<0.05

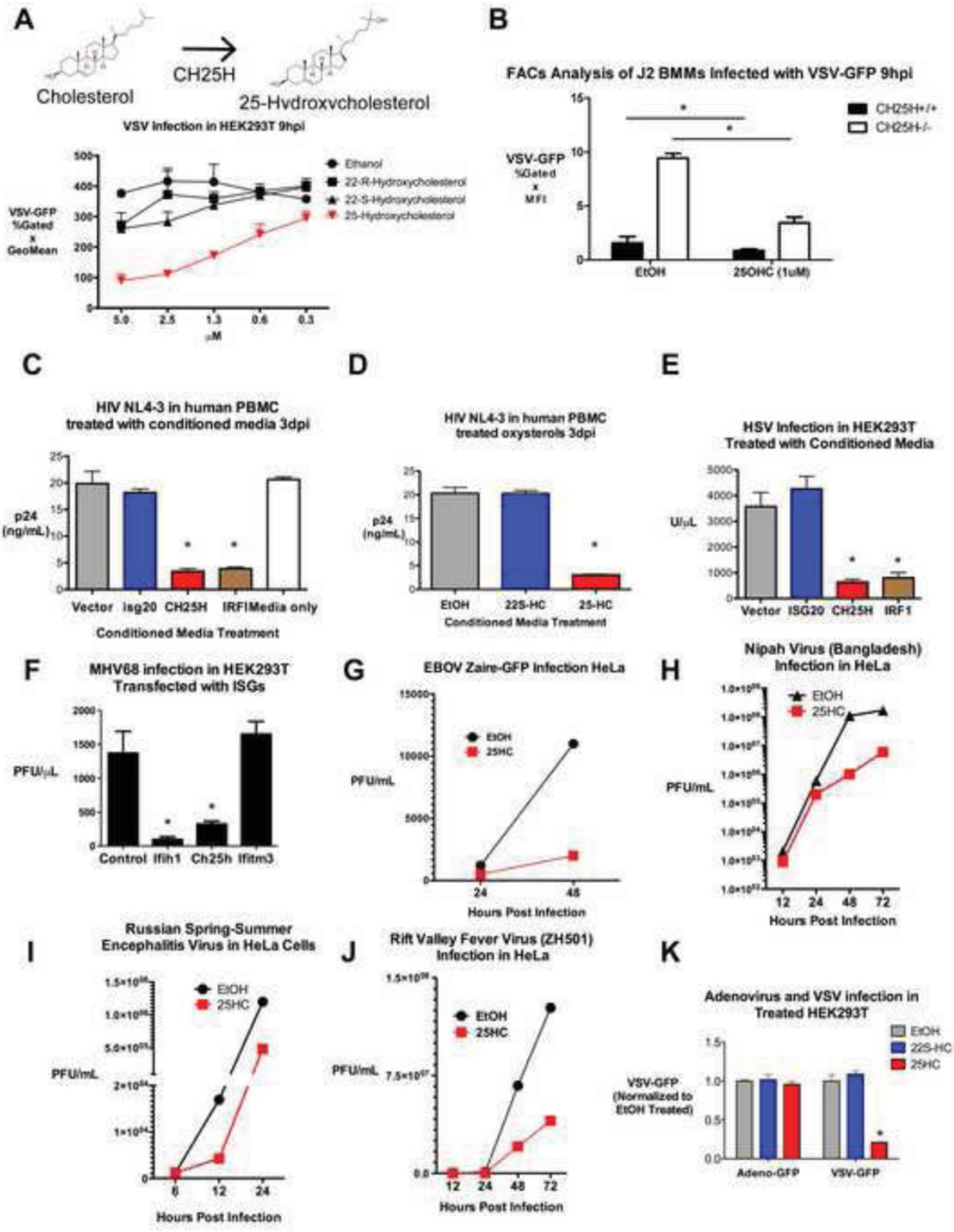

Figure 4. Ch25h produces 25-hydroxycholesterol, an oxysterol with broad antiviral properties

A) CH25H converts cholesterol to 25-hydroxycholesterol (25HC, top). HEK293T was treated with 22(S)-HC, 22(R)-HC, 25HC, and the vehicle, ethanol (EtOH) for 8h at the indicated concentrations and infected with VSV-GFP. VSV-GFP was quantified by FACs (%GFP+ X Geometric MFI).

B) *Ch25h+/+* and *Ch25h−/−* J2 BMMs were treated with 25HC(1μM) or EtOH and infected with VSV-GFP (0.01MOI). VSV-GFP was quantified by FACs at 12hpi. Mean±SD; *P<0.02

C) Costimulated PBMC were pre-incubated for 24h in conditioned media before infection with HIV NL4-3. At 3dpi, p24 in triplicate samples were quantified by ELISA. Mean±SEM; *P<0.001

D) Costimulated PBMC (1×10^6) were pre-incubated for 24h in 22(S)-HC (1μM), 25HC(1μM), and vehicle (EtOH) containing media before infection with HIV NL4-3 in triplicates (30 ng of HIV strain NL4-3). At 3dpi, p24 was quantified by ELISA. Mean ±SEM; *P<0.001

E) HEK293T was treated with indicated conditioned media for 12h and infected with HSV (0.25MOI) for 24h. HSV titer in the supernatant was quantified by plaque assay. Mean ±SEM; *P<0.001

F) HEK293Ts were transfected with indicated expression plasmids and infected with MHV68 (0.2MOI) for 24h. MHV68 titer in the supernatant was quantified by plaque assay. Mean±SEM; *P<0.001

G) HeLa cells were pretreated with 25HC (1μM) or EtOH containing media for 5h and infected with Ebola Zaire-GFP (EBOV) at 0.1MOI. At the indicated times, combined supernatants from biological triplicates was measured by plaque assay.

H) HeLa cells were pretreated with media containing indicated concentrations of 25HC or EtOH for 18h and infected with Nipah virus at 0.1MOI. At the indicated times, combined supernatants from biological triplicates was measured by plaque assay.

I) HeLa cells were pretreated as in Fig. 4H and infected with RSSEV at 0.1MOI. At the indicated times, combined supernatants from biological triplicates was measured by plaque assay.

J) HeLa cells were pretreated with media containing indicated concentrations of 25HC or EtOH for 5h and infected with wildtype Rift Valley Fever Virus ZH501 (RVFV) at 0.1MOI. Viral titer at indicated time points was measured by plaque assay. Values represent means of samples from triplicates.

K) HEK293T were treated with EtOH, 22S-HC, and 25HC for 12h and infected with adenovirus-GFP and VSV-GFP and quantified by FACs (%GFP+ X Geometric MFI). Mean ±SEM; *P<0.001

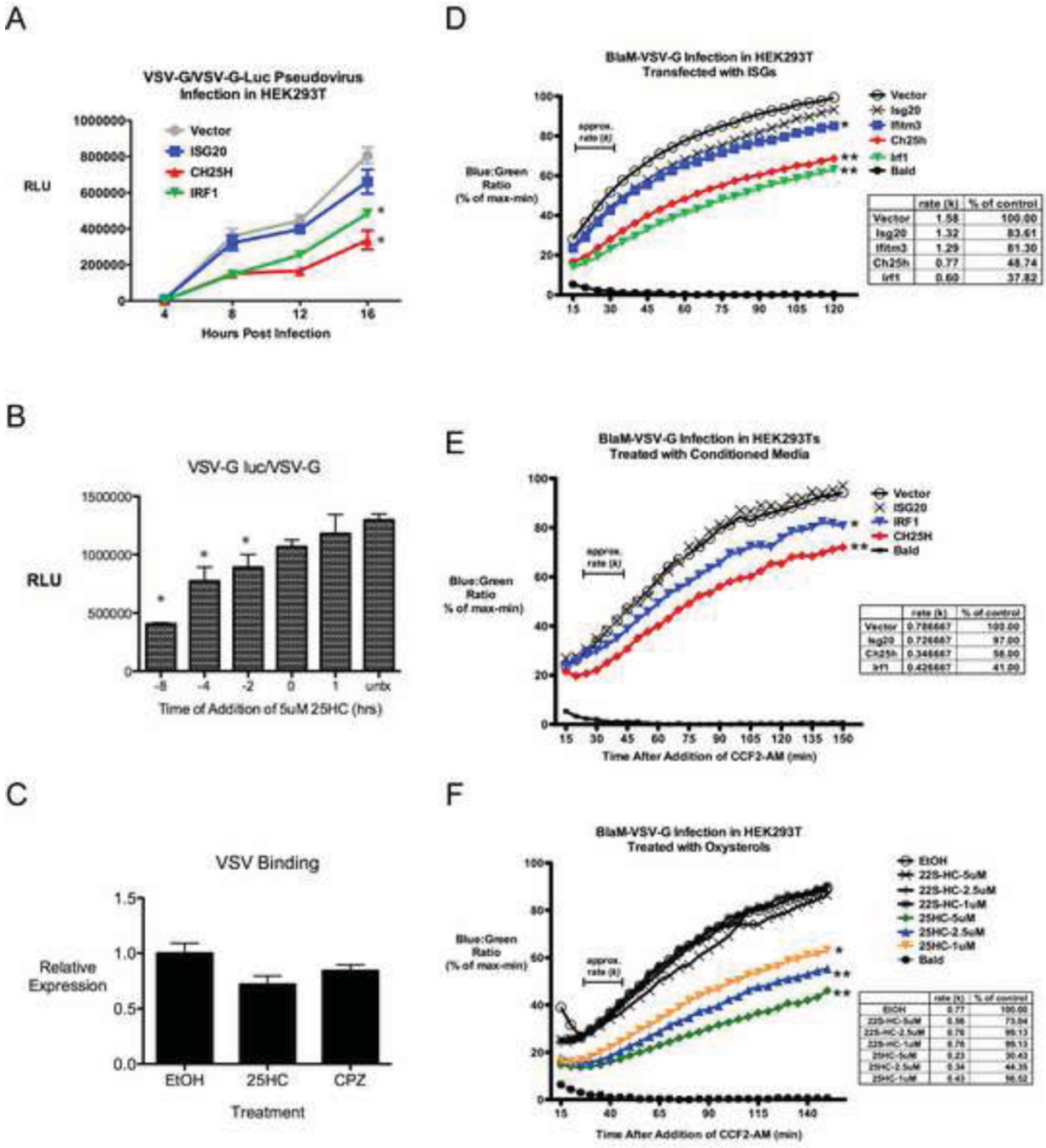

Figure 5. Ch25h-induced 25HC inhibits VSV Entry

A) HEK293Ts were treated with conditioned media for 12h and infected with VSV-G pseudovirus encoding VSVΔG luciferase (VSVΔG-Luc/G). The cell lysates were collected at indicated times and measured for luciferase activity.

B) HEK293T were treated with 25HC (5μM) at different times relative to the VSVΔG-Luc/G infection. For time 0, VSVΔG-Luc/G and 25HC were added together to the cells for 1h. Negative numbers indicate addition of 25HC before infection; positive number indicates addition after infection. Relative Light Units (RLU) is represented as Mean±SD *P<0.01

C) HEK293T were treated with respective agonists for 8h in triplicates. VSV was bound to cells at 4°C, washed 3 times with PBS, and let sit for 30min before total RNA collection. VSV genomic RNA was quantified by qRT-PCR Mean±SEM; *P<0.05

D) HEK293T was transfected with indicated expression plasmids for 24h and infected with pseudovirus with encoding NipahM-β-lactamase inside VSV-G (VSV-G/βlaM) for 1.5h. βla activity was measured by blue:green ratio of the cleaved CCF2-AM. The rate constant (k) (table, inset) estimated from the slope of the reactions in the bracketed time interval measures relative fusion. *P<0.01, **P<0.001

E) HEK293T was treated with indicated conditioned media for 12h and infected with VSV-G/βlaM. Analysis was same as part D. *P<0.01, **P<0.001

F) HEK293T was treated with indicated concentration of 22(S)-HC, 25HC, and equivalent volume of vehicle (EtOH) for 12h and infected with VSV-G/βlaM. Analysis was same as part D. *P<0.01,**P<0.001

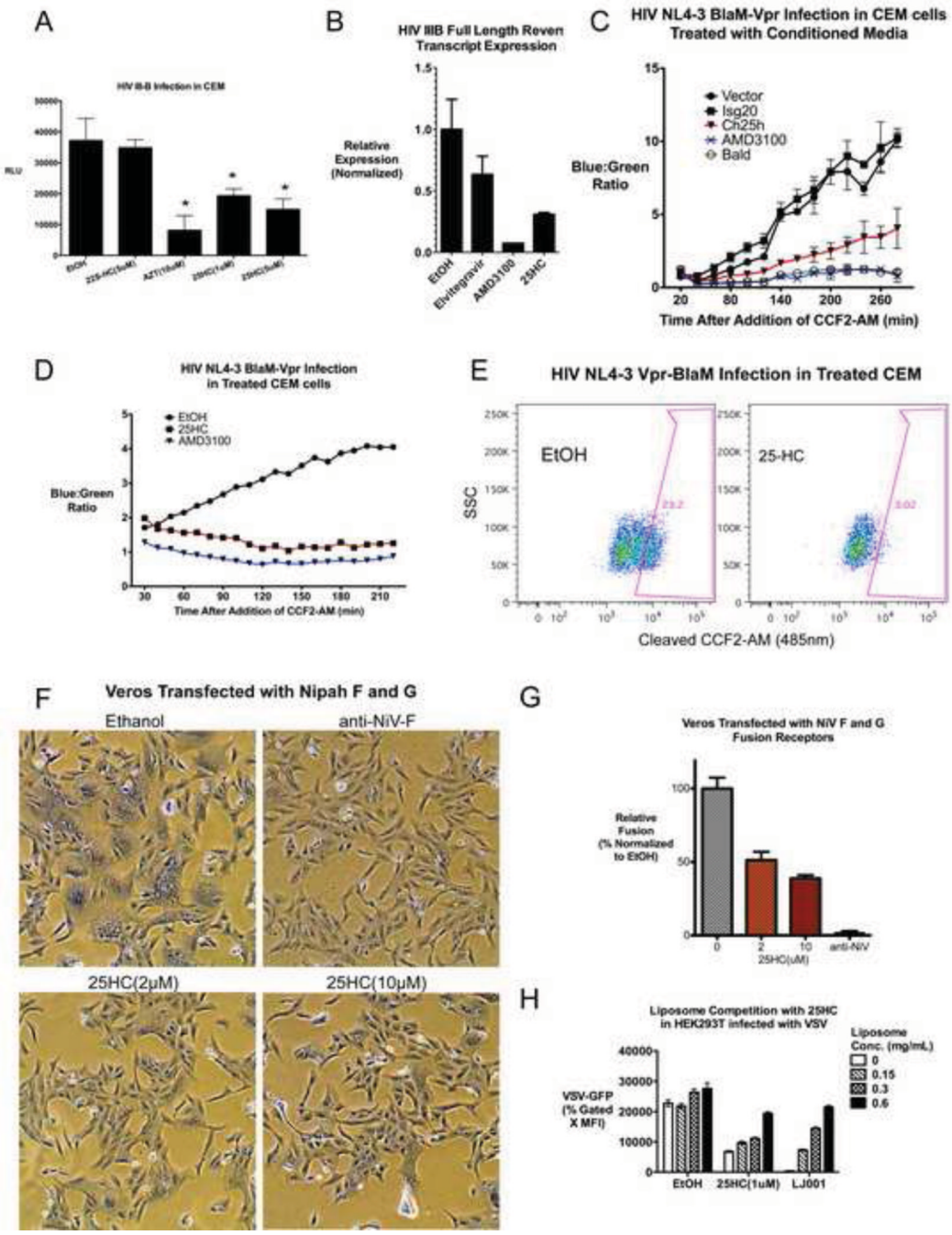

Figure 6. 25HC inhibits HIV Entry and Viral-Cellular Membrane Fusion

A) CEM cells were treated as indicated for 12h and underwent single-round infection with HIV-IIIB coexpressing luciferase. Cell lysates were collected after 24h and measured for luciferase activity. Relative Light Units (RLU) is represented as Mean±SD. *P<0.05

B) CEM cells were treated with elvitegravir (10μM), AMD3100(10μM), 25HC (1μM), and vehicle (EtOH) for 12h and infected with HIV III-B pseudovirus. At 6 hpi, HIV full-length late reverse transcript (LateRT) was quantified by qRTPCR with Taqman probe and normalized to mitochondrial DNA.

C) CEM cells were treated with indicated conditioned media or AMD3100 for 8h and infected with HIV NL4-3 encoding Vpr-βlaM (NL4-3/βlaM) in duplicates. βla activity was

measured by cleavage of CCF2-AM by fluorescence plate reader. Mean±SD *P<0.01 by student's t-test for last time point.

D) Similar to Part C. CEM cells were treated with indicated 25HC(5μM) and vehicle (EtOH) for 12h and infected with HIV NL4-3/βlaM.

E) After kinetic assay in Fig. 6D., percent of cleaved CCF2-AM (blue) population (485nm) was confirmed by FACs.

F) Vero cells were transfected with Nipah F and G receptors. 5h after transfection, the cells were treated with indicated conditions. The cells were fixed 21h after transfection and Giemsa stained.

G) Syncytias were defined by the presence of 4 or more nuclei in a common cell membrane. Relative fusion was determined by normalizing the number of nuclei per syncytia under the experimental conditions to the vehicle (ethanol) treated group, set to 100%.

H) HEK293T was incubated with 25HC (1μM) or LJ001, and varying concentrations of PC:cholesterol (7:3) liposomes before infection with VSVGFP. VSV-GFP was quantified by FACs.

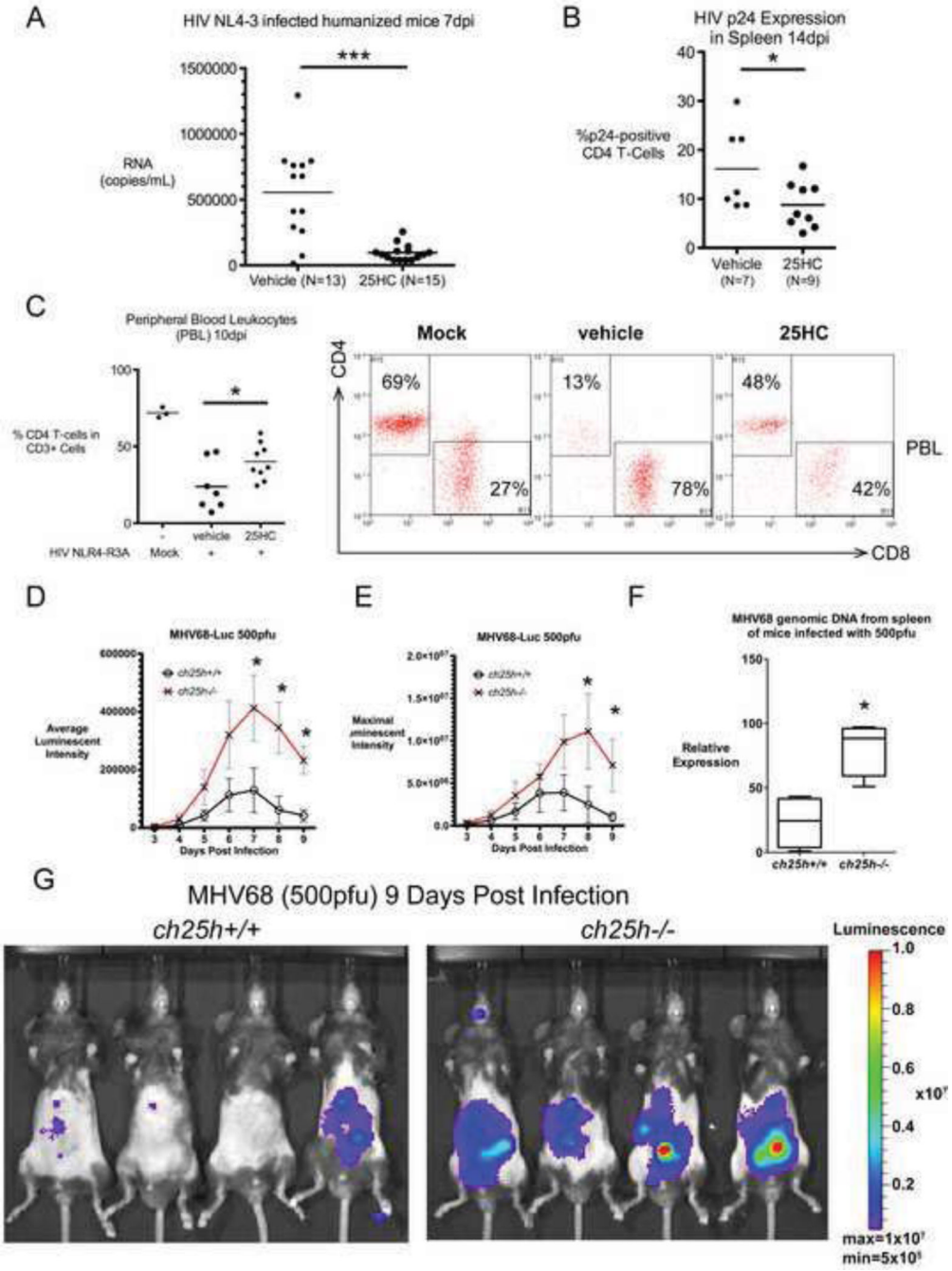

Figure 7. 25HC inhibits HIV replication and Ch25h is required for antiviral immunity *in vivo*

A) 25HC (50mg/kg) or vehicle (2-hydroxypropyl-β-cyclodextrin) was administered 12h before HIV NL4-3 infection in humanized mice (NRG-hu). Treatment was administered daily after infection. Viral titer in serum was measured by qRT-PCR 7dpi. Results are combined from 2 experiments. ***P<0.0001

B) Spleens from NRG-hu mice were harvested 14dpi and quantified by FACs after HIV p24 intracellular staining. *P<0.05

C) Percent CD4+ T-cells was compared by FACs in 25HC and EtOH treated group. Representative FACs plots are shown (right). *P<0.05

D) *ch25h+/+* and *ch25h−/−* mice were infected with MHV68-Luc (500pfu) and the amount of infection was quantified everyday by bioluminescence imaging. Average intensities (photons/sec/cm^2/steradian) from ventral, right, left, and dorsal sides were measured for all mice. *P<0.05 by student's t-test at indicated timepoint.
E) Similar to Fig. 7D, maximum intensities (photons/sec/cm^2/steradian) were averaged. *P<0.05 by student's t-test at indicated timepoint.
F) MHV68 genomic DNA from *ch25h+/+* and *ch25h−/−* infected mice 9dpi was quantified by qRT-PCR and normalized to a genomic promoter of ccl2 gene. *P<0.01
G) Bioluminescent images of *ch25h+/+* and *ch25h−/−* mice 9dpi.